JOURNAL OF THERMOPHYSICS AND HEAT TRANSFER
Vol. 11, No. 2, April–June 1997

Pool Boiling Curve in Microgravity

Ho Sung Lee* and Herman Merte Jr.†
University of Michigan, Ann Arbor, Michigan 48109-2125
and
Francis Chiaramonte‡
NASA Lewis Research Center, Cleveland, Ohio 44135

Pool boiling experiments using R-113 were conducted in the microgravity of space on a flat heater, consisting of a semitransparent gold film sputtered on quartz substrate, 19.05 × 38.1 mm (0.75 × 1.50 in.). Transient measurements of both the mean heater surface temperature and input heat flux are used to compute the mean heat transfer coefficient at the heater wall. Steady-state pool boiling is achieved in microgravity under conditions in which a large vapor bubble somewhat removed from the heater surface is formed, which acts as a reservoir for the nucleating bubbles. The steady nucleate boiling heat transfer is enhanced materially in microgravity relative to that in Earth gravity, whereas the heat flux at which dryout occurs is considerably less. Using quasisteady data obtained during periods in which some significant portions of the heater surface were dried out, it was possible to construct two distinct composite approximate microgravity pool boiling curves for R-113, one for the higher level of subcooling and one for the lower level of subcooling. These are compared with a reference curve for pool boiling at $a/g = +1$, constructed from available data and correlations deemed to reasonably represent the circumstances present.

Nomenclature

P_{sys} = system pressure
q''_T = total heat flux applied
T = temperature
T_{bulk} = bulk temperature
T_{sat} = saturation temperature
T^*_w = mean heater surface temperature at nucleation
t = time
t^* = delay time between onset of heating and nucleation
ΔT_{sub} = bulk liquid subcooling
ΔT_w = steady mean heater surface superheat
ΔT^*_w = mean heater surface superheat at nucleation

I. Introduction

POOL boiling can be viewed as the lower limit of forced convection boiling in microgravity and should be reasonably well understood, in terms of describing its behavior, as an initial step toward understanding the velocity effects on boiling. This can lead to an improved description of forced convection boiling in Earth gravity, not withstanding the current interest in its behavior in microgravity. A related intrinsic question with pool boiling in microgravity is whether a long-term steady state can be attained. This becomes a ponderable issue in the absence of appropriate experimental demonstrations. Pool boiling has been studied extensively in Earth gravity and disagreements are still in evidence as to the true nature of the source of enhancement in heat transfer, whether it is caused by latent heat transport, microconvection, or some combination. Since buoyancy performs a major role in pool boiling in Earth gravity, its absence in microgravity understandably leads to speculation about other mechanisms coming to the forefront.

One of the difficulties in experimentation is that of producing a microgravity environment on Earth. Prior experiments involving boiling in reduced gravity have been conducted and reported by Usiskin and Siegel,[1] Merte and Clark,[2] Siegel and Keshock,[3] Littles and Walls,[4] Oker,[5] Straub et al.,[6] Ervin et al.,[7] Merte et al.,[8] and Abe et al.,[9] using various facilities; parabolic aircraft flights, sounding rockets, and free fall in drop towers. The results to date have been contradictory: Usiskin and Siegel,[1] Merte and Clark,[2] and Straub et al.[6] have indicated that nucleate boiling heat transfer appears to be insensitive to reductions in gravity, whereas the results presented by Littles and Walls,[4] Oker,[5] Abe et al.,[9] and Merte et al.[8] demonstrate an enhancement of such boiling heat transfer in microgravity. It is believed that the geometry of the heater surface used is a major factor in the differences observed. In general, experiments conducted with wires indicate little or no change in nucleate boiling heat transfer in reduced gravity or microgravity compared to Earth gravity,[10] whereas flat surface heater surfaces tended to show somewhat of an improvement in microgravity.[11] The study of boiling on a ribbon in a drop tower by Siegel and Keshock[3] included both heat transfer measurements and high-speed photography. Although the heat transfer results were inconclusive with respect to the effect of reduced gravity, the observations that the small vapor bubbles formed at the heater surface and absorbed by coalescence with larger bubbles hovering nearby, led these authors to conclude that the stirring action and turbulence induced by the growth of these small bubbles can provide good heat transfer performance, even in the absence of buoyancy. The ramifications of this behavior can be extended in that the removal of these small bubbles by absorption by the larger ones can prevent dryout and sustain the mechanism of nucleate boiling in microgravity, a conclusion that can only be confirmed by long-term experiments. The variable quality of the gravity in the works referred to previously, as well as the short times available, render problematic the resolution of the apparent contradictions about the role of gravity up to the present time.

The purpose of this investigation is to provide experimental data for pool boiling under relatively long periods of micro-

Presented as Paper 96-0499 at the AIAA 34th Aerospace Sciences Meeting and Exhibit, Reno, NV, Jan. 15–19, 1996; received July 24, 1996; revision received Nov. 26, 1996; accepted for publication Nov. 29, 1996.

*Research Investigator, Department of Mechanical Engineering and Applied Mechanics, 2026 G. G. Brown.

†Professor, Department of Mechanical Engineering and Applied Mechanics, 2148 G. G. Brown. Member AIAA.

‡Aerospace Engineer, Microgravity Fluid Physics Branch, M/S 500-102.

gravity, using space flights and well-defined conditions, and to present the results in the form of the familiar pool boiling curve for comparison with the behavior in Earth gravity. An attempt is made to describe the mechanisms of pool boiling in microgravity by means of photographic visualization, with due consideration to the effects of heater surface size. Pool boiling experiments were conducted on three space flights, designated as PBE-IA-IB-IC on the STS-47, -57, and -60, respectively, as part of the NASA Get Away Special (GAS) program, with each flight experiment consisting of nine different test runs, conducted during 1992–1994. The identical test runs were repeated in Earth gravity following the space experiments so that direct comparisons could be obtained between the behavior in microgravity and in Earth gravity.

II. Experimental Apparatus and Procedure

Measurements of heat transfer and various parameters associated with bubble growth dynamics were obtained in the microgravity of space, providing on the order of $a/g \sim 10^{-4}$, with R-113. Nine test runs were conducted at three levels of heat flux (2, 4, and 8 W/cm^2) and three levels of subcooling (0, 2.7, and 11°C), each lasting up to 2 min, in each of three space experiments, for a total 27 test runs. Photographs of the boiling process were obtained simultaneously from the side and from beneath the heater surface at framing rates of 10 and 100 fps with a 16-mm cine camera. The three space experiments were virtually identical, differing primarily in the speeds and lengths of the photography and heating times. The same hardware was used for PBE-IA and IC (STS-47 and -60, respectively), whereas that of the PBE-IB (STS-57) was of the same construction. This provided opportunities for observations of repeatability and/or reproducibility, to be addressed briefly in the following text.

A. Test Vessel

Figure 1 presents a schematic diagram of the test vessel, consisting of R-113 and nitrogen (N_2) chambers. The R-113 chamber has internal dimensions of 15.2 cm diameter by 10.2 cm high and includes a gold film heater on a quartz substrate, a pressure transducer, thermistors, and stirrer. The stirrer functions to provide a timely uniform fluid temperature between each test. The pressure transducer measures the system pressure with an uncertainty of ±0.345 kPa, while thermistors measure the liquid temperatures adjacent to the heater surface at distances of 1, 5, and 10 mm, and at various other locations,

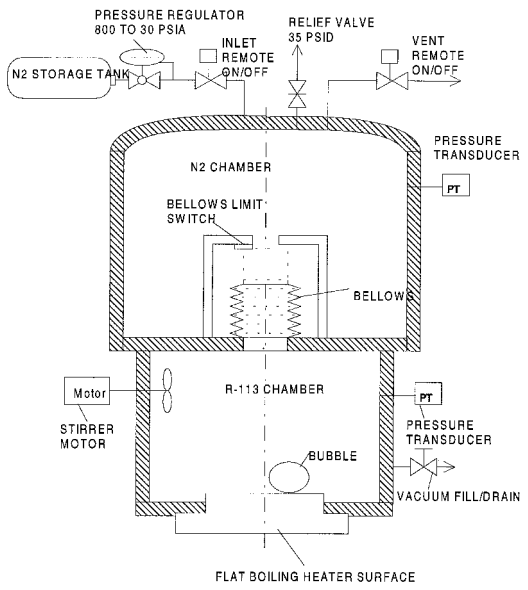

Fig. 1 Schematic of test vessel with concepts to provide constant pressure and initially uniform fluid temperature.

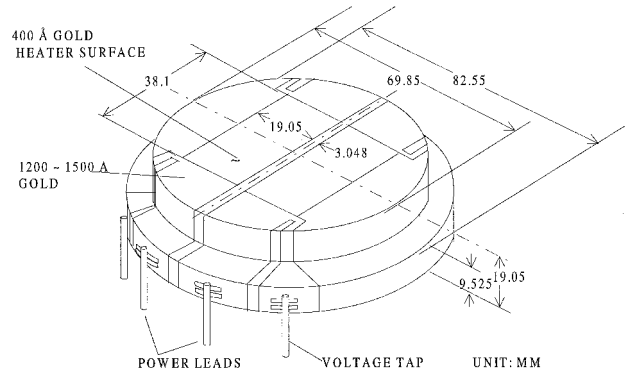

Fig. 2 Transparent gold film heater/resistance thermometer on quartz substrate.

with a total uncertainty of ±0.06°C. The nitrogen chamber is used to maintain the desired system pressure. System subcooling is obtained by increasing the system pressure above the saturation pressure corresponding to the initial liquid temperature. In the absence of buoyancy, an initially motionless liquid remains stagnant upon heating until the onset of boiling, and the temperature distribution in the liquid at the onset of boiling can be determined from a conduction heat transfer analysis.

B. Heater Surfaces

Two heater surfaces are placed on a single flat substrate, installed to form one wall of the test vessel as shown in Fig. 1, with one acting as a backup. Each heater consists of a 400-Å-thick semitransparent gold film sputtered on a highly polished quartz substrate (Fig. 2), and serves simultaneously as a heater, with an uncertainty of ±2% in the measurement of the heat flux, and a resistance thermometer, with an overall uncertainty of ±1.0°C. The heater is rectangular in shape, 19.05 × 38.1 mm (0.75 × 1.5 in.). Degassed commercial-grade R-113 (trichlorotrifluoroethane, CCl_2FCClF_2) was used because of its low normal boiling point (47.6°C), which minimized problems associated with heat loss to the surroundings, and because of its electrical nonconductivity, which is compatible for direct contact with the thin gold film heater. Further experimental details may be found in Ref. 12.

C. Measurement of Mean Heater Surface Temperature

Measurement of the electrical resistance across the heater surface provided the mean heater surface temperature as a function of time, with the aid of calibrations carried out prior to the experiments. These temperatures were filtered to remove noise effects, using a three-consecutive-point-averaging technique, advancing sequentially one point at a time, which serves to smooth the data without eliminating physical behavior. The total heat flux input is transported into both the liquid and the quartz heater substrate, and the measured mean heater surface temperatures can be used to compute the heat flux to the quartz substrate using appropriate numerical computations. Subtracting this from the input heat flux provides the heat flux to the liquid and the transient mean heat transfer coefficient. The identical numerical method was applied consistently throughout to compute the mean heat transfer coefficient, and it was demonstrated that a consistent relationship was maintained between the relative and absolute values of the heat transfer coefficients so computed. It will be noted later that although the heat flux to the liquid is used to compute the heat transfer coefficients, the total imposed heat flux is used as appropriate to distinguish between the different heat flux levels.

D. Experimental Procedure

When the desired uniform bulk liquid temperature in the test vessel is attained by the combination of the stirrer and electric

heater strips on the exterior surfaces, the test run begins with the activation of measurements of the various local fluid temperatures and pressure. Power to the thin film heater surface is activated at 10 s simultaneous with the camera unit, and results in the growth of a thermal boundary layer at the heater surface, up to the onset of boiling. The activation/deactivation of the heater, camera, and stirrer motor depend on the details of the specific test matrix, with a test run lasting up to 120 s. A fixed sampling rate of 10 Hz is employed to measure the mean heater surface temperature, system pressure, and fluid temperatures throughout the experiments.

III. Results and Discussion

The present experiments represent a somewhat restricted number and combination of variables because of limitations in size, weight, power, and accessibility. Of the 27 test runs conducted under microgravity in the three separate space flights, true steady-state boiling was present in only 13, whereas the remainder exhibited a quasisteady or transient rise of heater surface temperature associated with various degrees of dryout. Quasisteady is used here in the sense that the measured rate of heater surface temperature change is sufficiently slow so that heat capacity effects can be neglected in the computation of the heat flux described earlier. The current study focuses on the circumstances of pool boiling in microgravity in which steady or quasisteady state exists, which permits the establishment of a so-called microgravity pool boiling curve. The phenomena of nucleation, established or steady nucleate boiling, and completely established dryout were found to be quite reproducible, for given conditions. Partial dryout occurred under certain combinations of heat flux and subcooling, and the mean heater surface temperature depended on the fraction of the surface dried out. Detailed descriptions of these are available in Ref. 12.

A visual comparison of typical pool boiling with the same heater surface in both Earth gravity and microgravity is presented in Fig. 3, where the upper half presents the side view and the lower half is the bottom view through the semitransparent gold film heater. The bright spots in the lower left are the binary time indicators. The operating conditions are almost identical for both the normal gravity and reduced gravity. Vapor bubbles in Earth gravity are observed to be quite small, compared to those in microgravity, because of buoyancy forces acting to remove the vapor bubbles from the vicinity of the heater surface. The numerous relatively larger bubbles in microgravity are uniformly distributed and attached to or in the vicinity of the heater surface. The mean heater surface superheats are 27°C in Earth gravity and 18.1°C in microgravity, which indicates an obvious enhancement of the heat transfer process in microgravity. This is presumed to be because of the evaporation of the larger liquid microlayer areas formed beneath the vapor bubbles in microgravity.

Measurements of the mean heater surface superheat with the derived mean heat transfer coefficient are presented in Fig. 4 as a function of time for the cases shown in Fig. 3. The measured mean heater surface superheats are observed to reach the steady-state levels within 5–10 s following nucleation. These cases will be considered in more detail later by examining photographs and measurements of both the local fluid temperature in the vicinity of the heater surface and the system pressure. It is noted in Fig. 4 that operation in a microgravity environment with these conditions results in an enhancement in the nucleate boiling heat transfer, manifested here by an increase in the mean heat transfer coefficient from h = 1250 W/m^2 K at $a/g = +1$ to h = 1650 W/m^2 K at $a/g = 10^{-4}$, an increase of about 32%. The mean heater surface superheat in microgravity rises to 62.8°C prior to nucleation by transient heat conduction, with a mean heat transfer coefficient of about 250 W/m^2 K. The attainment of such a high superheat at nucleation is believed to be a consequence of the smoothness of

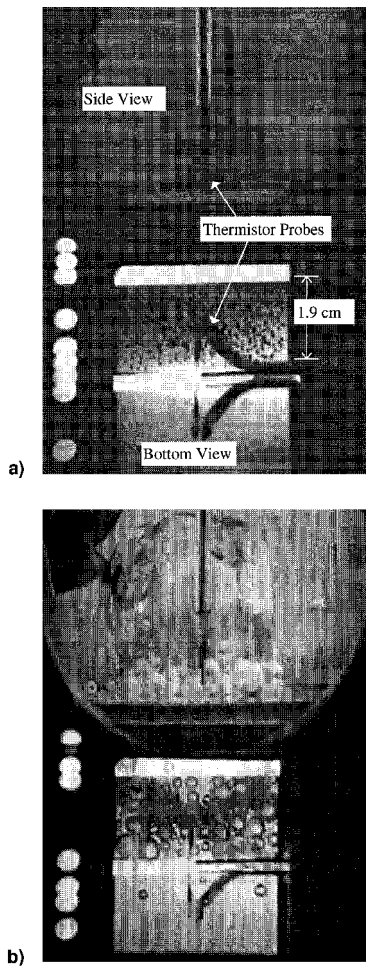

Fig. 3 Visual comparison of pool boiling with R-113 on earth and during a Space Shuttle flight under otherwise similar conditions. a) Normal gravity $a/g = +1$ (t = 78.22 s), postflight (STS-60) run no. 2: q''_T = 3.6 W/cm^2, P_{sys} = 150.1 kPa, ΔT_w = 27°C, ΔT_{sub} = 11.5°C. b) Reduced gravity $a/g = 10^{-4}$ (t = 61.47 s), space flight (STS-60) run no. 2: q''_T = 3.6 W/cm^2, P_{sys} = 145.9 kPa, ΔT_w = 18.1°C, ΔT_{sub} = 11.5°C.

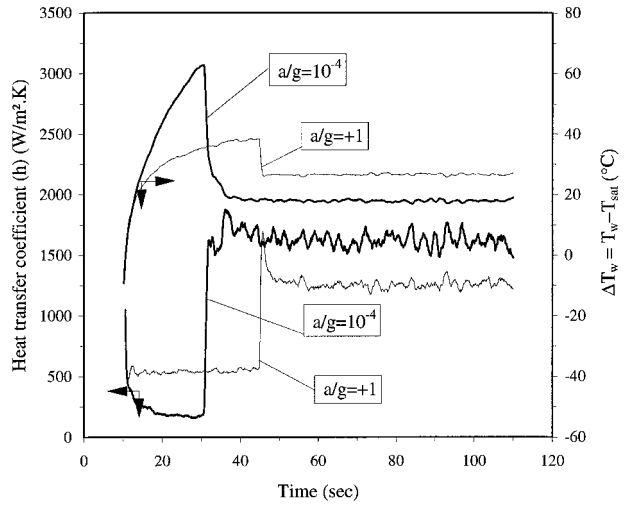

Fig. 4 Comparison of measured mean heater surface superheats and derived heat transfer coefficients between STS-60 run no. 2 and postflight (STS-60) run no. 2. Space flight (STS-60) run no. 2: $a/g = 10^{-4}$, t^* = 20.85 s, q''_T = 3.6 W/cm^2, P_{sys} = 145.9 kPa, T_{sat} = 58.9°C, T_{bulk} = 47.4°C, T_w = 77°C, ΔT_w = 18.1°C, ΔT_{sub} = 11.5°C. Postflight (STS-60) run no. 2: $a/g = +1$, t^* = 35.08 s, q''_T = 3.6 W/cm^2, P_{sys} = 150.1 kPa, T_{sat} = 59.9°C, T_{bulk} = 48.4°C, T_w = 86.9°C, ΔT_w = 27.0°C, ΔT_{sub} = 11.5°C.

the heater surface, resulting in what has been termed homogeneous nucleation.[13] The superheat curve in Earth gravity, on the other hand, rises slowly to 37.4°C, because of the natural convection, with a heat transfer coefficient of about 500 W/m^2 K, which is in good agreement with the natural convection correlation of Lloyd and Moran.[14]

The dynamic initial vapor bubble growth and subsequent steady pool boiling for the microgravity case in Fig. 4 are presented photographically in Figs. 5 and 6, respectively. The rapid drop in the mean heater surface temperature, at the maximum rate of 33°C/s, appears to be related to the evaporation of the thin liquid layer formed beneath the large bubble and the subsequent initial dynamic vapor bubble growth taking place, which impels the large vapor bubble away from the heater surface. Cooler liquid is then drawn beneath the large departing bubble, followed by the formation of new bubbles. These phenomena are shown in Fig. 5. The camera speed was not high enough to stop the vapor bubble motion, so that the bubble in Fig. 5a appears to be blurred. The bulk liquid pressure resulting from the dynamic growth is depicted in Fig. 7, where the peak pressure reaches 159.7 kPa at 30.8 s, preceded and followed by a constant pressure of 146 kPa. It becomes obvious that the pressure control system was not capable of responding to this disturbance. The absence of any pressure disturbance upon nucleation in Earth gravity should also be noted.

A. Vapor Bubble Coalescence and Removal

Figure 6 is a sequence of photographs of the steady-state pool boiling process in microgravity following the initial dynamic vapor bubble growth of Fig. 5, separated by intervals of about 10 s to present a more complete picture of pool boiling. What is notable here is that following nucleation the small bubbles grow at first by evaporation and then by coalescence with adjacent vapor bubbles, followed by sudden removal from the vicinity of the heater surface by coalescence with the large vapor bubble observed at the back edge of the heater. This is the bubble that was initially impelled away from the heater surface, and which now plays an important role in removing

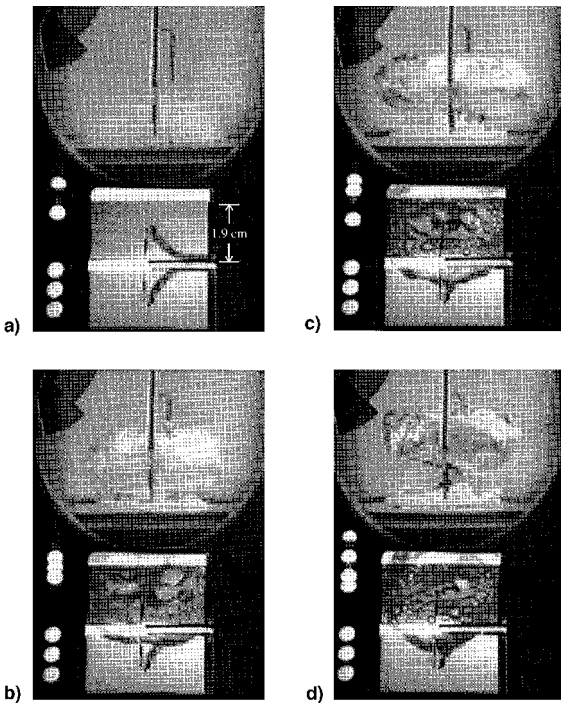

Fig. 5 Dynamic vapor bubble growth with R-113 in microgravity for STS-60 run no. 2. $a/g = 10^{-4}$, $t^* = 20.85$ s, $q''_T = 3.6$ W/cm^2, $P_{sys} = 145.9$ kPa, $T_{sat} = 58.9$°C, $T_{bulk} = 47.4$°C, $T^*_w = 122.7$°C, $\Delta T^*_w = 62.8$°C, $\Delta T_{sub} = 11.5$°C. Time = a) 30.85, b) 31.05, c) 31.25, and d) 31.55 s.

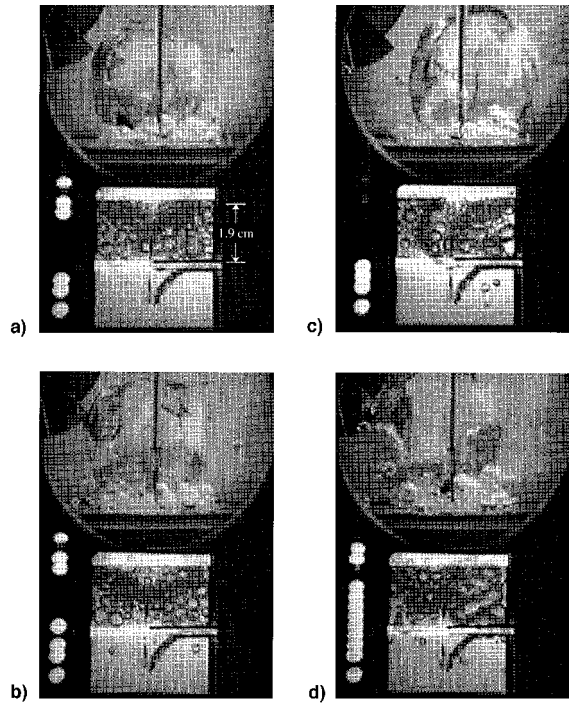

Fig. 6 Steady pool boiling in microgravity for STS-60 run no. 2. $a/g = 10^{-4}$, $q''_T = 3.6$ W/cm^2, $P_{sys} = 145.9$ kPa, $T_{sat} = 58.9$°C, $T_{bulk} = 47.4$°C, $T_w = 77$°C, $\Delta T_w = 18.1$°C, $\Delta T_{sub} = 11.5$°C. Time = a) 51.23, b) 61.47, c) 71.45, and d) 91.40 s.

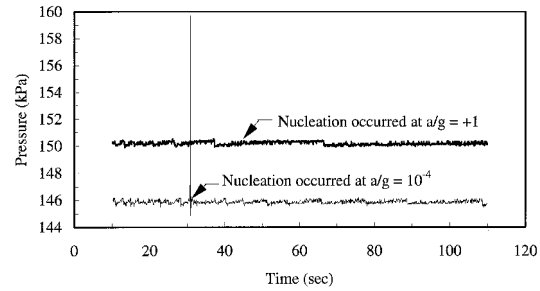

Fig. 7 System pressure measurement for space flight STS-60 run no. 2 and postflight (STS-60) run no. 2.

the newly formed vapor bubbles from the heater surface by surface tension, thereby inhibiting the onset of dryout of the heater surface. The cyclic repetition of the vapor bubble generation and coalescence process induces turbulence in the fluid adjacent to the heater surface, thereby enhancing the boiling heat transfer in microgravity. As pointed out earlier, a similar phenomenon was described by Siegel and Keshock[3] for a single bubble coalescence in reduced gravity, although it was not possible to determine the enhancement quantitatively because of the short experimental periods available at that time. Because of limitations in the camera speed and film length associated with the automation of the experiment, it was not possible to determine the frequency of formation of the small vapor bubbles at the heater surface.

The local fluid temperature measurements 1 mm above the heater surface are shown in Fig. 8 both at Earth gravity and during the space flight for run no. 2, corresponding to Figs. 3–7. These are expressed in terms of superheat, and the consistent bulk heating occurring in microgravity prior to nucleation is quite obvious, followed by oscillations between the saturation temperature corresponding to the system pressure of Fig. 7 and a subcooling of approximately 2°C, representing the variations between the saturated vapor of the local bubbles and the bulk liquid being transported toward the heater surface. In Earth gravity on the other hand, oscillations arise because of

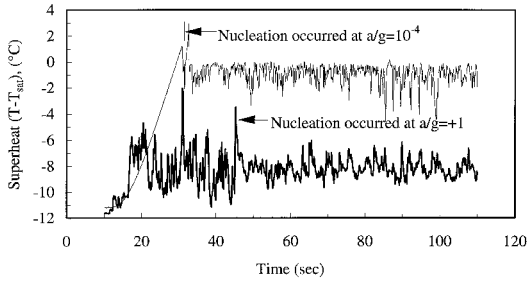

Fig. 8 Local fluid superheat ($T - T_{sat}$) measured at 1 mm above the heater surface for space flight STS-60 run no. 2 and postflight (STS-60) run no. 2.

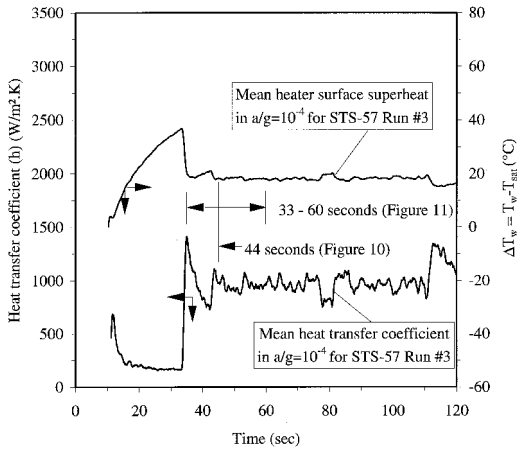

Fig. 9 Measured mean heater surface temperature and derived heat transfer coefficient for STS-57 run no. 3: $a/g = 10^{-4}$, $t^* = 23.63$ s, $q''_T = 2.0$ W/cm^2, $P_{sys} = 149.3$ kPa, $T_{sat} = 59.7$°C, $T_{bulk} = 48.7$°C, $T_w = 78$°C, $\Delta T_w = 18.3$°C, $\Delta T_{sub} = 11.5$°C.

single-phase natural convection prior to nucleation, followed by continuous oscillations between subcoolings of 6–9°C.

The coalescence of vapor bubbles at the heater surface in microgravity can be seen more readily at the lowest nominal heat flux level of 2 W/cm^2. The mean heater surface temperature and heat transfer coefficients are given in Fig. 9 for STS-57 run no. 3, whereas the coalescence is illustrated visually in Fig. 10. The photographs show several pairs of vapor bubbles coalescing on contact because of surface tension, increasing in size and reducing in number by half during a period of 0.06 s. The vapor bubbles attached to the heater surface undergo rapid movements as a result of the coalescence, inducing corresponding motions in the fluid adjacent to the heater surface. These relatively large vapor bubbles are then absorbed by the large bubble residing above the heater surface, which acts as a reservoir. After absorption the heater surface is rewetted and the cycle is repeated. The enhancement of boiling heat transfer in microgravity is attributed to this sequence of events. Abe et al.[9] and Straub et al.[6] have attempted to describe the heat transfer with pool boiling in microgravity in terms of Marangoni convection. However, the present vapor bubble motion described previously appears to be so vigorous that effects of Marangoni convection on the heat transfer would be reduced. If the Marangoni convection were a significant force, the vapor bubble would be impelled toward the heater surface because of the temperature gradient. No comparisons were possible between the mean heat transfer coefficient in microgravity, about 1000 W/m^2 K at $a/g = 10^{-4}$ in Fig. 9, and in Earth gravity because nucleation did not occur at $a/g = +1$ at the low heat flux level of 2 W/cm^2. It was observed that the bubble motions become more vigorous in microgravity as the heat flux increases, as also occurs in Earth gravity.

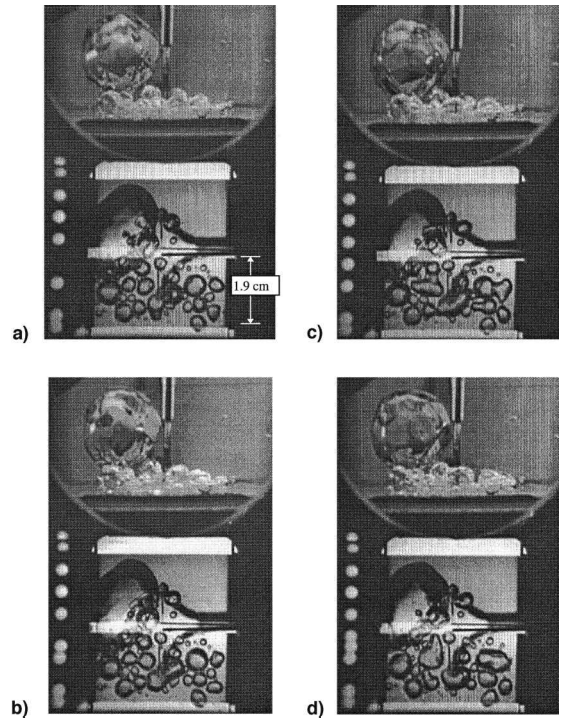

Fig. 10 Vapor bubble coalescence for STS-57 run no. 3: $a/g = 10^{-4}$, $q''_T = 2.0$ W/cm^2, $P_{sys} = 149.3$ kPa, $T_{sat} = 59.7$°C, $T_{bulk} = 48.7$°C, $T_w = 78$°C, $\Delta T_w = 18.3$°C, $\Delta T_{sub} = 11.5$°C. Time = a) 44.16, b) 44.18, c) 44.20, and d) 44.22 s.

B. Heater Surface Dry Fraction

The computed mean heat transfer coefficient is quite sensitive to changes in the mean heater surface temperature, as can be noted in Fig. 9, and after viewing the photographs of the boiling process from the heater underside, the question arises as to whether a direct relationship exists between changes in the heater surface temperature and the heater surface dry fraction, that portion of the heater surface that is not wet. During those intervals when a distinct portion of the heater surface was dry, the dry area was measured frame by frame using an image process software, from which the heater surface dry fraction was determined. Measurements of the dry ratio for STS-57 run no. 3, whose data and photographs are given in Figs. 9 and 10, are plotted in Fig. 11 over the time interval of 33–60 s along with the corresponding mean heater surface temperature. It is noted that a direct correspondence exists between the variation of the mean heater surface temperature and the dry ratio. As a result, the increase in the mean heater surface temperature taking place over the time interval of 35–43 s in Fig. 11 can be attributed directly to the increase in partial dryout of the heater surface.

From detailed analysis of the 27 test runs conducted in microgravity in the three space experiments to this point, the quasisteady nucleate boiling defined previously always took place for the cases in which the two lower heat flux levels of 2 and 4 W/cm^2 and the high subcooling level of 11°C were present. Transient dryout always occurred at the high heat flux level of 8 W/cm^2 at all levels of subcooling used here. A representative case of transient dryout in microgravity is shown in Fig. 12, together with the steady nucleate boiling in Earth gravity for similar conditions in STS-60 run no. 4. At the high heat flux level of 6.5 W/cm^2 and the subcooling of 3.2°C, the mean heater surface superheat in microgravity increases to about 160°C at 45 s, whereas in Earth gravity the steady boiling results in a heat transfer coefficient of about 2400 W/m^2 K. On considering all tests in microgravity it is determined that dryout [or critical heat flux (CHF)] for R-113 occurs at heat flux levels between 6.5–3.6 W/m^2 K.

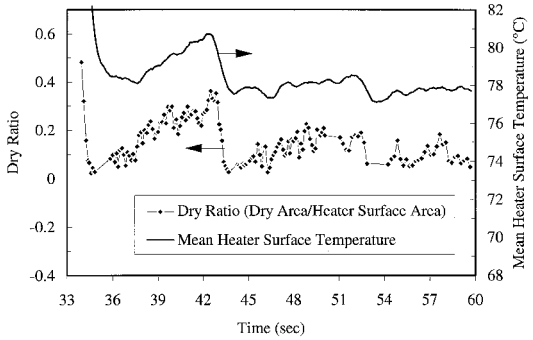

Fig. 11 Heater surface dry fraction and mean heater surface temperature correlation for STS-57 run no. 3.

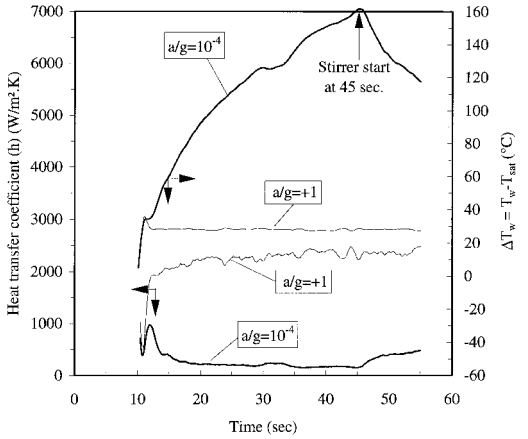

Fig. 12 Comparison of measured mean heater surface superheat and derived heat transfer coefficient between space flight STS-60 run no. 4 ($a/g = 10^{-4}$) and postflight (STS-60) run no. 4 ($a/g = +1$). Space flight (STS-60) run no. 4: $a/g = 10^{-4}$, $t^* = 0.74$ s, q''_T = 6.5 W/cm², P_{sys} = 117.3 kPa, T_{sat} = 52.0°C, T_{bulk} = 48.8°C, T_w = dryout, ΔT_w = dryout, ΔT_{sub} = 3.2°C. Postflight (STS-60) run no. 4: $a/g = +1$, $t^* = 0.76$ s, q''_T = 7.0 W/cm², P_{sys} = 114.1 kPa, T_{sat} = 51.1°C, T_{bulk} = 47.9°C, T_w = 79.1°C, ΔT_w = 28°C, ΔT_{sub} = 3.2°C.

Of the total of 12 test runs at both the two lower levels of subcooling and the two lower levels of heat flux, 7 test runs resulted in quasisteady nucleate boiling, with no degree of consistency with the parameters of heat flux and subcooling used. The large bubble initially formed on the heater surface either moved away from the heater surface or remained attached, producing partial dryout of the surface, depending on the intensity of the initial dynamic vapor bubble growth. As described earlier, the large bubble then can serve as a reservoir to absorb and remove the bubbles generated at the heater surface, and permit the heater surface to be maintained in a wetted condition, producing in turn the quasisteady nucleate boiling, even with low levels of subcooling. In this latter case the large bubble continuously grows until contact is made with the opposite surface, inducing subsequent dryout at the heater surface. A typical test run at both a lower level of subcooling (0.8°C) and heat flux (1.8 W/m²), which demonstrates this behavior, is illustrated in Fig. 13. The mean heater surface superheat is quite steady, even with a low subcooling close to saturation. Steady boiling appears to be possible in principle, with a saturated liquid, provided that a large bubble remains in residence near the heater surface such that a sufficient flow of liquid would still take place to all parts of the heater surface. This latter requirement would probably place an upper limit on the size of a flat heater surface that could sustain nucleate pool boiling in microgravity.

Direct comparisons between nucleate pool boiling at $a/g = +1$ and microgravity with identical systems are given in Fig. 14. Also included are the measurements of Oker[5] obtained with

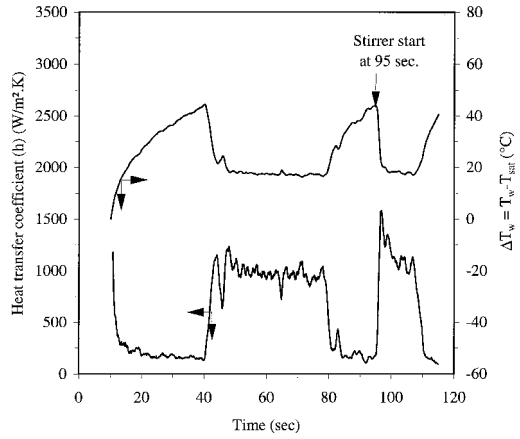

Fig. 13 Measured mean heater surface superheat and derived heat transfer coefficient for space flight (STS-60) run no. 9: $a/g = 10^{-4}$, $t^* = 30.52$ s, q''_T = 1.8 W/cm², P_{sys} = 107.7 kPa, T_{sat} = 49.4°C, T_{bulk} = 48.6°C, T_w = 67.4°C, ΔT_w = 18°C, ΔT_{sub} = 0.8°C.

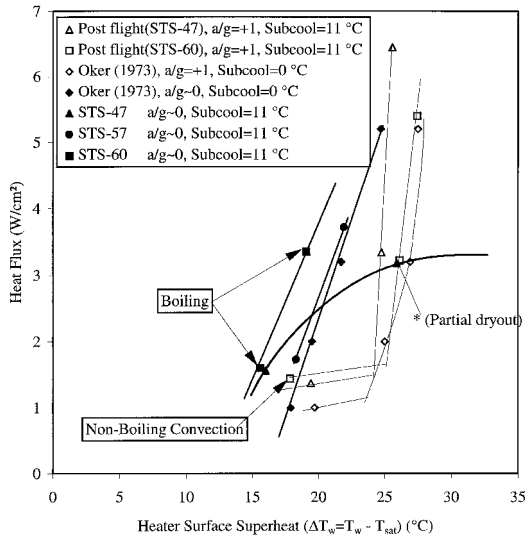

Fig. 14 Direct comparisons of nucleate pool boiling of R-113 between identical systems at $a/g = +1$ and microgravity conditions.

R-113 in a 1.4-s drop tower with $a/g < 10^{-3}$, giving a fair agreement with the present data. A gold film heater similar to the present heater was used. It is clear in all cases here that a significant and reproducible degree of enhancement in the boiling process of about 30% takes place at the lower levels of heat flux with some degree of subcooling. Although the majority of test runs in which partial dryout was present produced transient boiling processes, one quasisteady case existed with a partial dryout of about 25%, and is so indicated in Fig. 14. This occurred on STS-47 run no. 2 at a heat flux of 3.6 W/m² and 11°C subcooling, and resulted in an increased mean heater surface superheat to 26°C, as shown.

Based on observations of all microgravity testing conducted here, a general conclusion can be reached that, although subcooling has negligible influence on the steady microgravity heat transfer coefficient, increasing subcooling appears to increase the probability that such steady boiling will take place.

IV. Microgravity Pool Boiling Curve

Sufficient information appears to be available at the present time to permit a somewhat speculative construction of an approximate microgravity pool boiling curve. Two such curves are shown in Fig. 15, in which all available data for R-113 are plotted, including the quasisteady or short-term steady, and the slow transient, consisting of progressive dryout or rewetting.

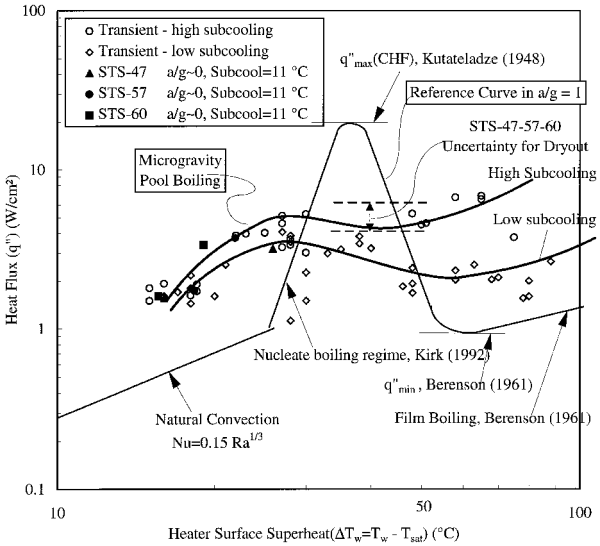

Fig. 15 Approximate composite microgravity pool boiling curves for R-113 from steady and quasisteady measurements on STS-47-57-60.

Also given in Fig. 15 is a composite reference curve for pool boiling at Earth gravity, constructed using available data and correlations that seem to be reasonably representative of the circumstances present.[15–17] The approximate composite microgravity pool boiling curve consists of two curves at this time; one for low levels of subcooling and the other for the higher level of subcooling used here, which bear some resemblance to the reference curve, albeit over a wider spread in the heater surface superheat. The uncertainty of the heat flux at which dryout takes place is estimated to be within the range of 4–6 W/cm^2, as shown in Fig. 15.

Pool boiling with fluids whose wetting characteristics are unlike that of R-113, and with surfaces different from the highly polished quartz used, could produce behavior different from that described here.

V. Conclusions

It appears that long-term steady-state nucleate boiling can take place on a flat heater surface in microgravity with a wetting liquid under conditions in which a large vapor bubble somewhat removed from the heater surface is formed, which acts as a reservoir to remove the bubbles from the immediate vicinity of the heater surface. The steady nucleate boiling heat transfer is significantly enhanced in microgravity compared to that in Earth gravity.

Surface tension has an important role in producing dryout and/or rewetting on a heated surface. The detailed circumstances describing this remain to be explored, but the heat flux at which dryout occurs is considerably less in microgravity than in Earth gravity.

Using the quasisteady data obtained during the periods in which some significant portions of the heater surface were dried out, it was possible to construct two distinct composite approximate microgravity pool boiling curves for R-113, one for the higher level of subcooling and one for the lower level of subcooling. This is compared with a reference curve for pool boiling at $a/g = +1$, constructed from available data and correlations deemed to reasonably represent the circumstances present. The microgravity pool boiling curves bear some resemblance to the reference curve, although the maximum heat flux (critical heat flux) is reduced considerably. The minimum (film boiling) heat flux, corresponding to complete dryout in microgravity, can also be anticipated to be reduced considerably below that in Earth gravity.

Acknowledgment

This work was supported, with appreciation, under NASA Contract NAS 3-25812.

References

[1]Usiskin, C. M., and Siegel, R., "An Experimental Study of Boiling in Reduced and Zero Gravity Fields," *Journal of Heat Transfer*, Vol. 83, No. 3, 1961, pp. 243–253.

[2]Merte, H., Jr., and Clark, J. A., "Boiling Heat Transfer with Cryogenic Fluid at Standard, Fractional, and Near-Zero Gravity," *Journal of Heat Transfer*, Vol. 86C, 1964, pp. 315–319.

[3]Siegel, R., and Keshock, E. G., "Effects of Reduced Gravity on Nucleate Boiling Bubble Dynamics in Saturated Water," *AIChE Journal*, Vol. 10, No. 4, 1964, pp. 509–517.

[4]Littles, J. W., and Walls, H. A., "Nucleate Pool Boiling of Freon 113 at Reduced Gravity Levels," *Proc. Fluid. Eng., Heat Transfer and Lubr. Conference*, American Society of Mechanical Engineers, 70-HT-17, New York, 1970.

[5]Oker, E., "Transient Boiling Heat Transfer in Saturated Liquid Nitrogen and R113 at Standard and Zero Gravity," Ph.D. Dissertation, Univ. of Michigan, Ann Arbor, MI, 1973.

[6]Straub, J., Zell, M., and Vogel, B., "Pool Boiling in a Reduced Gravity Field," *Proceedings of the 9th International Heat Transfer Conference* (Jerusalem, Israel), Vol. 1, Hemisphere, New York, 1990, pp. 91–112.

[7]Ervin, J. S., Merte, H., Jr., Keller, R. B., and Kirk, K., "Transient Pool Boiling in Microgravity," *International Journal of Heat and Mass Transfer*, Vol. 35, No. 3, 1992, pp. 659–674.

[8]Merte, H., Jr., Lee, H. S., and Ervin, J. S., "Transient Nucleate Pool Boiling in Microgravity—Some Initial Results," *Microgravity Science Technology*, Vol. VII/2, 1994, pp. 173–179.

[9]Abe, Y., Oka, T., Mori, Y. H., and Nagashima, A., "Pool Boiling of a Non-Azeotropic Binary Mixture Under Microgravity," *International Journal of Heat and Mass Transfer*, Vol. 37, No. 16, 1994, pp. 2405–2413.

[10]Straub, J., "The Role of Surface Tension for Two-Phase Heat and Mass Transfer in the Absence of Gravity," *Experimental Thermal and Fluid Science*, Vol. 9, 1994, pp. 253–273.

[11]Merte, H., Jr., "Combined Roles of Buoyancy and Orientation in Nucleate Pool Boiling," *Collected Papers in Heat Transfer 1988-Vol. 2*, HTD-Vol. 104, Annual Meeting of American Society of Mechanical Engineers, Nov. 1988.

[12]Merte, H., Jr., Lee, H. S., and Keller, R. B., "Report on Pool Boiling Experiment Flown on STS-47-57-60," Dept. of Mechanical Engineering and Applied Mechanics, Univ. of Michigan, Rept. UM-MEAM-95-01, NASA Contract NAS 3-25812, Ann Arbor, MI, 1995.

[13]Merte, H., Jr., and Lee, H. S., "Homogeneous Nucleation in Microgravity at Low Heat Flux: Experiments and Theory," American Society of Mechanical Engineers, Paper 95-WA/HT-41, Nov. 1995.

[14]Lloyd, J. R., and Moran, W. R., "Natural Convection Adjacent to Horizontal Surface of Various Platforms," *Journal of Heat Transfer*, Vol. 96C, No. 4, 1974, pp. 443–447.

[15]Kirk, K. M., "A Study of the Relative Effects of Buoyancy and Liquid Momentum in Forced Convection Nucleate Boiling," Ph.D. Dissertation, Univ. of Michigan, Ann Arbor, MI, 1992.

[16]Kutateladze, S. S., "On the Transition to Film Boiling Under Natural Convection," *Kotloturbostroenie*, No. 3, 1948, p. 10.

[17]Berenson, P. J., "Film Boiling Heat Transfer from a Horizontal Surface," *Journal of Heat Transfer*, Vol. 83, 1961, p. 351.